processes

Article

New Model for Non-Spherical Particles Drag Coefficients in Non-Newtonian Fluid

Jiankun Liu [1,2], Zhaokai Hou [3,*], Guoqing Xu [1,2] and Lipeng Yan [1,2]

1 State Key Laboratory of Shale Oil and Gas Enrichment Mechanisms and Effective Development, Beijing 102206, China
2 Sinopec Research Institute of Petroleum Engineering Co., Ltd., Beijing 102206, China
3 College of Petroleum Engineering, Northeast Petroleum University, Daqing 163318, China
* Correspondence: houzk@nepu.edu.cn

Abstract: The settlement drag coefficient of non-spherical particles (SDCNPs) is a crucial parameter in the field of petroleum engineering. Accurately predicting the SDCNPs in the fluid is essential to the selection and design of proppant and hydraulic design in the fracturing scheme. Although many models for anticipating the SDCNPs have been proposed, none of them can be adopted for non-Newtonian fluid (NNF) and Newtonian fluid (NF). In the investigation, the SDCNPs in NF and NNF are studied experimentally, and the anticipation mode of the settlement drag coefficient of spherical particles (SDCSPs) in different fluids (including Newton, Herschel-Bulkley and power law) is proposed. On this basis, the shape depiction parameter circularity is introduced to develop the SDCNPs. The results exhibit that the predicted values of the SDCNPs model perfectly align with the experimental values, and the average relative errors are 5.70%, 6.24% and 6.72%, respectively. The mode can accurately describe the settlement behavior of non-spherical particles (NSPs) and provide a basis for the application of NSPs in petroleum engineering.

Keywords: non-spherical particles; drag coefficient; non-Newtonian fluid; settlement experiment; circularity

Citation: Liu, J.; Hou, Z.; Xu, G.; Yan, L. New Model for Non-Spherical Particles Drag Coefficients in Non-Newtonian Fluid. *Processes* **2022**, *10*, 1990. https://doi.org/10.3390/pr10101990

Academic Editor: Andreas Håkansson

Received: 8 September 2022
Accepted: 28 September 2022
Published: 2 October 2022

1. Introduction

The particle sedimentation phenomenon widely exists in nature and is widely used in industry [1,2]. The study of particle settling velocity (PSV) is a classical problem in petroleum engineering. PSV is a key parameter in petroleum engineering applications. For example, proppant placement efficiency in fracturing and prediction of solid concentration distribution in mud pipelines are related to particle settling velocity [3]. The accurate calculation of particle settlement velocity depends on its settlement drag coefficient (C_D). Therefore, accurate prediction of particle settlement drag coefficient is of great significance for construction parameter optimization and equipment design, and has attracted a large number of researchers to study it.

In the early research, scholars mainly studied the settlement drag coefficient of spherical particles (SDCSPs) in Newtonian fluid (NF). As early as 1851, Stokes [4] established an anticipation formula for the drag coefficient (DC) of spherical particles (SPs) in NF. However, this formula is only applicable to cases with a low Reynolds number. For the higher Reynolds number of particles, the result obtained by using Stokes drag formula has a large error. Subsequently, Abraham [5], Clift [6], Brown [7] and Terfous [8], respectively, established C_D-Re_N correlations under different Reynolds numbers (Re_N). Agwu [9], Goossens [10] and Shanshan Yao [11], respectively, summarized the C_D-Re_N correlation of spherical particles in NF.

Compared with the research work of SPs in Newtonian fluid (NF), less attention is paid to the settling behaviour of SPs in non-Newtonian fluid (NNF). In the early stage, Chhabra [12], Lali [13], kelesidis [14] and others believed that the SDCSPs were independent of the fluid rheology, so the calculation formula of the settlement drag coefficient of particles

(SDCPs) in NF can be directly applied to non-Newtonian fluid. With the deepening of research, Subhash [15] and James [16] believe that the particle settling drag coefficient (SDC) constitutes a role of Reynolds number (RN) and a function of flow pattern index n. Kelesidis [17], Turton [18], Haider [19], Cheng [20], Song [21], okesanya [22] and Khan [23] proposed different C_D-Re_N correlations based on the fluidity index of non-Newtonian fluids. In addition, for viscoelastic fluids, they have both shear thinning and considerable elasticity. Zhang [24] and padhy [25] proposed C_D-Re_N correlation for viscoelastic fluids by comprehensively considering the shear thinning and elasticity of polymer solutions.

The SDCPs is impacted not only by the rheological property of the fluid, but also by its shape. For irregular particles, scholars have proposed some concepts to characterize the particle shape features, like roughness [26], sphericity [27], circularity [28], Corey shape factor [29] and combined shape factor [30]. On this basis, Hölzer [31], Yin Wang [32], Chien [33], Fabio [34], Xu and others [35], respectively, put forward C_D-Re_N relations, which is applicable to irregular-shaped sand particles. In addition, other methods have also been used to calculate the SDCNPs. The artificial intelligence-based machine learning algorithm is used by Rushd [36] and Barati [37] to predict the SDCNPs in different fluids. Akanni [38] and Gavrilov [39] used numerical simulation methods to calculated the SDCNPs. Zhou [40] and Okesanya [41] used imaging measurements to measure the SDCNPs and established the SDCNPs model.

At present, most liquids employed in petroleum engineering are NNFs (mainly power-law fluids and Herschel-Bulkley fluids). Although many calculation models of particle settling drag coefficient have been proposed, there is no one that can be adopted to NF and NNF. In addition, common proppant and rock debris are irregular shapes, so it is necessary to use the shape factor to correct C_D-Re_N. Sphericity is the most widely used geometrical parameter. However, the sphericity constitutes a function of the particle surface area while it's hard to determine the sphericity of the particles with highly irregular shapes such as rock debris, which leads to a large error in calculating the settlement velocity using the sphericity. Therefore, how to accurately depict non-spherical particle irregularity and establish the corresponding C_D-Re_N correlation is an urgent problem to solve in the fluid field.

In this study, the SDCs of SPs and irregular sand particles in NF and NNF are comprehensively analyzed and experimentally studied. Based on the classical empirical model, a general mathematical formula is established for anticipating the SDC of non-spherical particles (SDCNPs) in NNF through introduction of the 2D shape description parameter circularity (c), sensitive to particle profile irregularity and easy to determine. The established model may better depict the settling behaviour of non-spherical particles (NSPs) in NNF. The investigation is crucial to anticipating the SDC of irregular shaped particles in NNFs in petroleum engineering, enriching the research content of solid-liquid two-phase flow and perfecting the multiphase flow theory.

2. Research Methods

2.1. Testing Materials and Fluid Rheology

Four different concentrations of glycerol, seven different concentrations of carboxymethyl cellulose (CMC) and five different concentrations of carbomer aqueous solution were selected as experimental fluids. After mixing glycerol, CMC and carbomer with water, seal for at least 24 h. After the bubbles escape, test the rheological parameters of different fluids with an advanced rheometer (Anton Paar MCR 92). Figures 1–3 show rheological curves of different flui; it can be seen from the figure that the three aqueous solutions are, respectively, typical NF, power-law fluid and Herschel-Bulkley fluid.

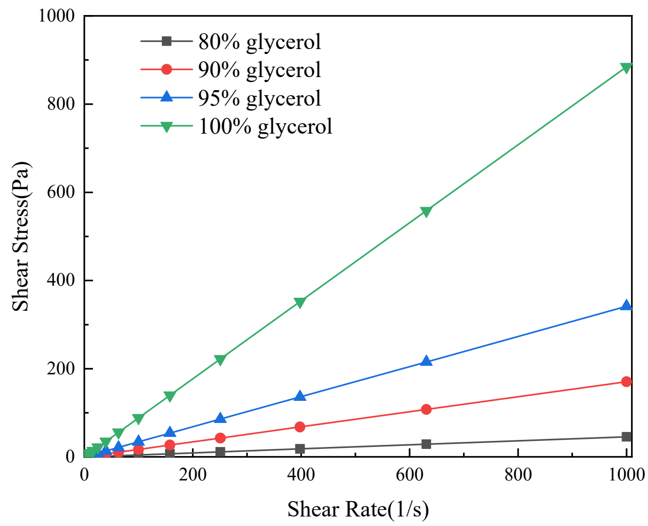

Figure 1. Rheological plots of glycerol aqueous solutions with different concentrations.

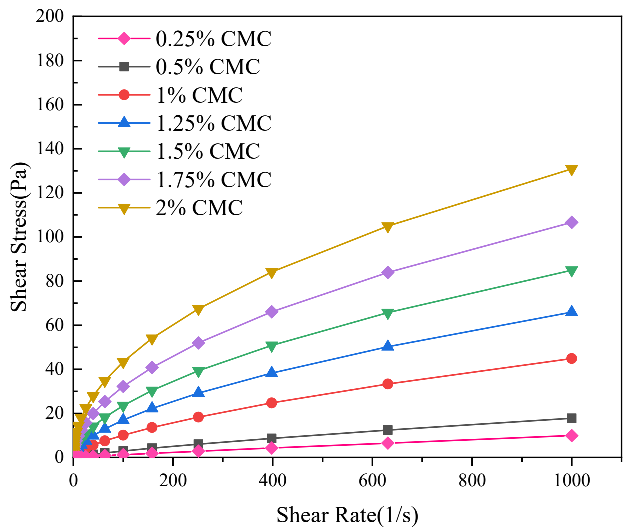

Figure 2. Rheological curves of CMC aqueous solutions with different concentrations.

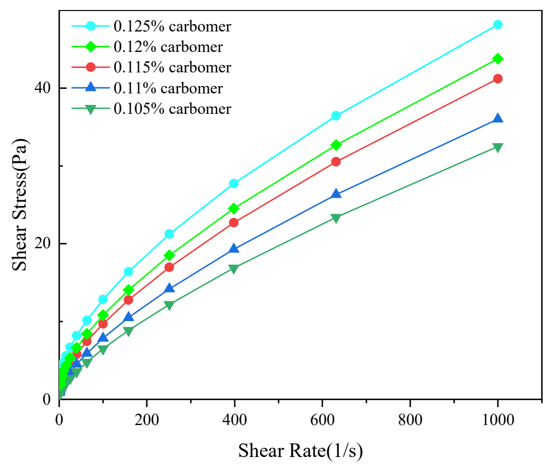

Figure 3. Rheological curves of carbomer aqueous solutions with different concentrations.

The corresponding constitutive equations of Newton, Herschel-Bulkley and Power-law fluids (PLFs) are exhibited in Table 1.

Table 1. Common fluid rheological models.

Rheological Models	Equation
Newton	$\tau = \mu_B \gamma$
Power law	$\tau = k\gamma^n$
Herschel-Bulkley	$\tau = \tau_0 + k\gamma^n$

Where τ represents the shear stress, Pa; τ_0 denotes the yield value, Pa. γ represents the shear rate, 1/s; K denotes the fluid consistency coefficient, Pa·s^n.

Fitting the rheological curves in Figures 1–3 with the constitutive model in Table 1, we can obtain the consistency index K and fluidity index n (Table 2).

Table 2. Rheological parameters of different fluids.

Test Fluids	Temperature, (°C)	Density, kg/m^3	Rheological Parameters		
			τ_0, Pa	K, Pa·s^n	n
80 wt % glycerol	24.3	1210	0	0.04562	1
90 wt % glycerol	22.1	1220	0	0.17059	1
95 wt % glycerol	24.5	1240	0	0.34144	1
100 wt % glycerol	22.9	1250	0	0.88462	1
0.25 wt % CMC	20.3	1001.5	0	0.0199	0.8986
0.5 wt % CMC	20.2	1001.5	0	0.0815	0.7797
1 wt % CMC	20.9	1003	0	0.5144	0.6470
1.25 wt % CMC	21.3	1003.2	0	1.1256	0.5891
1.5 wt % CMC	22.1	1004	0	1.8128	0.5569
1.75 wt % CMC	21.4	1004.5	0	2.9310	0.5203
2 wt % CMC	20.0	1006	0	4.7803	0.4791
0.105 wt % carbomer	23.9	1000	0.5041	0.2111	0.7268
0.11 wt % carbomer	24.3	1000	0.8363	0.2803	0.6995
0.115 wt % carbomer	23.9	1000	1.2990	0.3757	0.6754
0.12 wt % carbomer	23.6	1000	1.6841	0.4304	0.6634
0.125 wt % carbomer	23.6	1000	2.4108	0.5432	0.6418

2.2. Measurement of Particle Shape Factor

The SP materials adopted in the experiment are glass, zirconia and stainless steel. The density is 7930 kg/m^3, 6080 kg/m^3 and 2500 kg/m^{3,} respectively, and the particle diameter is 1–5 mm. Using different materials is mainly to expand the Reynolds number range of particles.

In this study, white quartz sand particles (see Figure 4) are selected as the sedimentation experiment of non-spherical particles, featuring a density of 2650 kg/m^3 and an equivalent diameter of 1.64–5.8 mm.

At present, circularity c is the simplest one among many shape factors that describe particle irregularity. Circularity c refers to the ratio of the maximal projection surface circumference of the particle to its equivalent circle circumference; it's a 2D shape parameter, and its formula is:

$$c = \frac{\pi d_A}{P_p} \quad (1)$$

in which d_A represents the diameter of the equivalent circle of the maximal projection plane of the particle, m; P_p denotes the maximum projection surface perimeter of the particle, m.

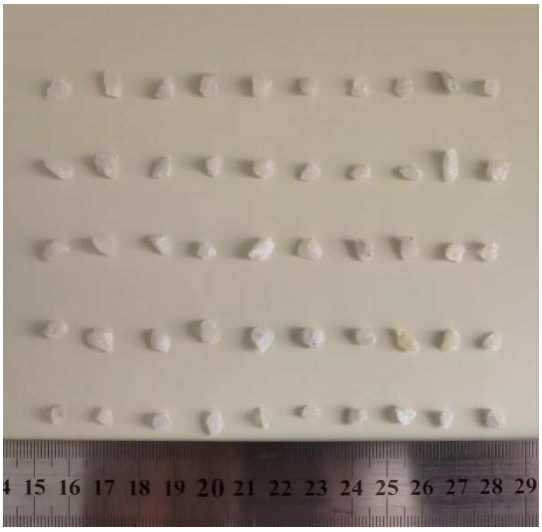

Figure 4. Physical properties of natural sand.

Circularity is sensitive to the particle profile irregularity and easy to measure. Therefore, circularity C is more suitable to be introduced into the settlement drag coefficient model. The measurement of circularity requires to process the image with the image processing commercial software ImageJ (Version 1.53c), ImageJ is open source software which is developed by the National Institutes of Health. Figure 5 shows a conversion example of an irregular shaped sand image. In the image processing process, the digital image (Figure 5a) captured by the camera is first converted into an 8-bit grayscale image as shown in Figure 5b). Then, the gray threshold approach is employed for identifying the particle edge (Figure 5c). During the identification process, the confirmed particle edge is made for coinciding with the original particle edge as much as possible, and the circularity is finally determined (Figure 5d).

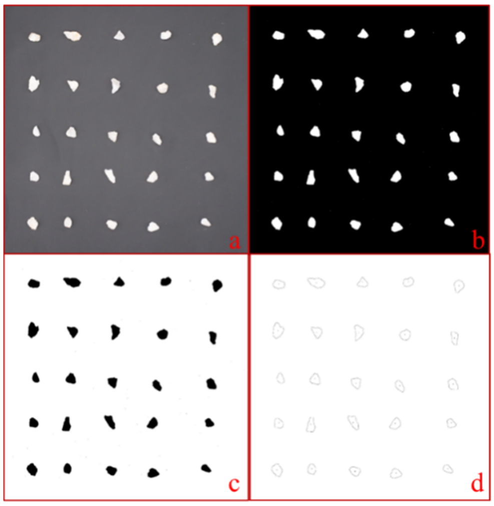

Figure 5. Conversion example of irregular sand image: (**a**) Original RGB image; (**b**) Converted into an 8-bit grayscale image; (**c**) Thresholding of images; (**d**) Draw profile.

2.3. Experimental Equipment and Procedures

Carry out the particle sedimentation experiment in a transparent plexiglass cylinder featuring a height of 1800 mm and an inner diameter of 100 mm. Use a high-speed camera for capturing the sedimentation course. The photos of the sedimentation experiment device are exhibited in Figure 6. Various contents of carbomer aqueous solution, CMC and glycerol solution should be prepared before the experiment, and stirred for more than 8 h with a mixer to fully dissolve them. Pour the experimental fluid into the organic glass inner tube and let it stand for 12 h to make the gas in the fluid fully escaped and stabilize the internal flow field. To ensure good solid-liquid contact, immerse the experimental particles in the experimental fluid and allow them to stand for more than 24 h, so that the particle surface is fully wetted and the surface gas is fully escaped, so as to eliminate the influence of the physical interaction between the experimental fluid and the particle surface on the particle settling speed during the settling experiment.

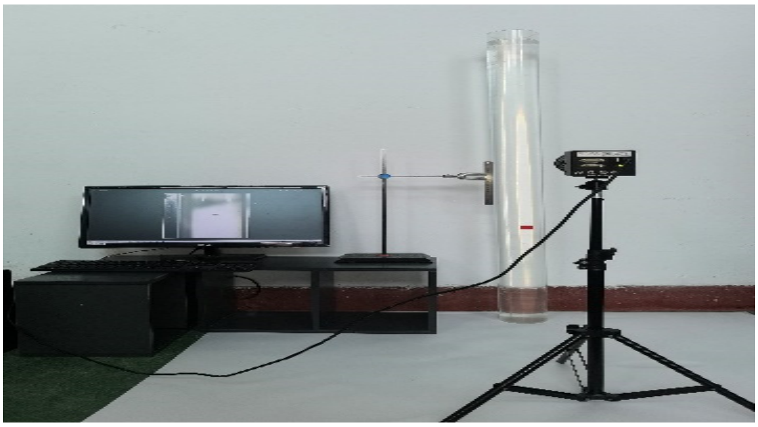

Figure 6. Particle sedimentation test equipment.

Place the experimental particlesbelow the liquid surface of the vertical pipe for making them freely settle along the pipe center; use a high-speed camera for capturing the settling motion trajectory of particles in a circular tube, and multiple image frames of the particle motion trajectory at various times are acquired. Stay 5 min after each group of experiments to ensure the stability of the internal flow field before the next experiment, so as to eliminate the influence of the particle settling trail in the previous experiments on the next particle settling speed; Conduct three repeated measurements for each particle under the same settlement conditions to ensure that the average deviation of the three measurement results is less than 5%.

The position of the particles at different times is analyzed and processed by the graphics digitizing software GetData graph digitizer for determining the coordinates of the particles in each frame of image. The ratio of the particle displacement between two frames to the time interval is the particle settling velocity (PSV). Then, the settlement drag coefficient and particle RN can be calculated according to the corresponding settlement velocity correlation.

Generally, the SDCPs is usually calculated by Equation (2):

$$C_d = \frac{4(\rho_p - \rho_l) g d_e}{3 V_s^2 \rho_l} \tag{2}$$

where C_d is the settlement drag coefficient; g represent gravitational acceleration, m/s^2; d_e denotes the effective sedimentation particle size, m; V_s represents the settling speed of particles, m/s; ρ_P is particle density, kg/m^3; ρ_l denotes fluid density, kg/m^3.

When particles settle in fluids with different properties, particle Reynolds number (RN) expression is different. When particles settle in Newtonian fluid, the Reynolds number of particles is expressed as follows:

$$\mathrm{Re}_N = \frac{\rho_p V_s d_e}{\mu} \tag{3}$$

where Re_N represents the particle RN settling in Newtonian fluid, μ is the viscosity of Newtonian fluid, Pa·s.

When a particle settles in a PLF, the particle RN is expressed as follows:

$$\mathrm{Re}_N = \frac{\rho_p V_s^{2-n} d_e^n}{K} \tag{4}$$

If the particles settle in the Herschel-Bulkley fluid (HBF), the Reynolds number expression of particle is as follows:

$$\mathrm{Re}_N = \frac{\rho_p V_s^{2-n} d_e^n}{K + \tau_0 \left(\frac{d_e}{V_s}\right)^n} \tag{5}$$

where τ_0 represents the fluid yield value, Pa; K denotes the fluid consistency coefficient, Pa·s^n; n represents fluid fluidity index, dimensionless.

3. Results and Discussion

3.1. Drag Coefficient of SPs

Based on results of spherical particle sedimentation experiment, the C$_D$-Re$_N$ curves of different fluids are drawn in classical logarithmic coordinates (Figure 7). The figure also includes the predicted values of seven models such as Turton, Haider, brown, Cheng and others. The specific forms of different models are listed in Table 3. Experimental data of spherical particle sedimentation are consistent with the predicted values of existing models (Figure 7).

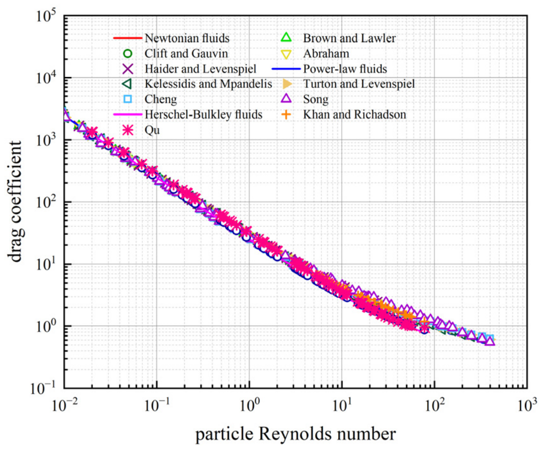

Figure 7. Relationship between spherical particle sedimentation experiment and predicted C$_D$-Re$_N$.

Table 3. C$_D$-Re$_N$ correlation of spherical particles settling in NF and NNF proposed by predecessors.

Reference	C$_D$-Re$_N$ Empirical Correlations
Abraham [5]	$C_D = \left(\sqrt{\frac{24}{\mathrm{Re}_N}} + 0.5407\right)^2$
Clift and Gauvin [6]	$C_D = \frac{24}{\mathrm{Re}_N}(1 + 0.15\mathrm{Re}_N^{0.687}) + \frac{0.42}{1+42500/\mathrm{Re}_N^{1.16}}$
Brown and Lawler [7]	$C_D = \frac{24}{\mathrm{Re}_N}(1 + 0.15\mathrm{Re}_N^{0.681}) + \frac{0.407}{1+8710/\mathrm{Re}_N}$
Kelessidis and Mpandelis [17]	$C_D = \frac{24}{\mathrm{Re}_N}(1 + 0.1407\mathrm{Re}_N^{0.6018}) + \frac{0.2118}{1+0.42150/\mathrm{Re}_N}$
Turton and Levenspiel [18]	$C_D = \frac{24}{\mathrm{Re}_N}(1 + 0.173\mathrm{Re}_N^{0.657}) + \frac{0.413}{1+16300/\mathrm{Re}_N^{-1.09}}$
Haider and Levenspiel [19]	$C_D = \frac{24}{\mathrm{Re}_N}(1 + 0.186\mathrm{Re}_N^{0.6459}) + \frac{0.4251}{1+6880.95/\mathrm{Re}_N}$
Cheng [20]	$C_D = \frac{24}{\mathrm{Re}_N}(1 + 0.27\mathrm{Re}_N)^{0.43} + 0.47[1 - \exp(-0.04\mathrm{Re}_N^{0.38})]$
Song [21]	$C_D = \frac{24}{\mathrm{Re}_N}(1 + 0.35\mathrm{Re}_N)^{0.44}$
Khan and Richadson [23]	$C_D = \left(2.25\mathrm{Re}_N^{-0.31} + 0.36\mathrm{Re}_N^{0.06}\right)^{3.45}$
Qu [42]	$C_D = \frac{24}{\mathrm{Re}_N}(1 + 0.282\mathrm{Re}_N^{0.229}) + \frac{167.28}{1-33000/\mathrm{Re}_N}$

In this study, root average squared logarithmic error (*RMSLE*), average relative error (*MRE*) and sum of the square errors (*SSE*) were used to evaluate the disparity between the experimental value and the anticipated one of the model. Calculation formulas of *MRE*, *RMSLE* and *SSE* are as follows:

$$MRE = \frac{1}{N}\sum_{i=1}^{N}\frac{|C_{DP,i} - C_{DM,i}|}{C_{DM,i}} \times 100\% \tag{6}$$

$$RMSLE = \sqrt{\frac{1}{N}\sum_{i=1}^{N}(\ln C_{DP,i} - \ln C_{DM,i})^2} \tag{7}$$

$$SSE = \frac{\sum_{i=1}^{N}(C_{DP,i} - C_{DM,i})^2}{\sum_{i=1}^{N}(C_{DM,i})^2} \tag{8}$$

where N represents the quantity of samples; C_{DP} denotes the settlement drag coefficient calculated by the model, dimensionless; C_{DM} is the settlement drag coefficient measured by experiments, dimensionless.

The error statistics between the experimental values of the SDCSPs in NF and NNF and the predicted values of previous models are shown in Table 4.

Table 4. Error statistics of SDCSPs in Newtonian fluid (NF) and non-Newtonian fluid (NNF).

Fluid Type	Correlation	Prediction Error (%)		
		MRE	*RMSLE*	*SSE*
Newtonian fluid	Brown and Lawler	3.41	4.10	0.14
	Clift and Gauvin	3.30	0.30	0.14
	Abraham	4.89	5.92	0.15
	Haider and Levenspiel	4.04	4.48	0.13
Power-law fluid	Kelessidis and Mpandelis	9.62	10.74	1.21
	Turton and Levenspiel	10.61	11.97	1.21
	Cheng	10.78	12.41	1.18
	Song	12.57	14.48	1.18
Herschel-Bulkley fluid	Khan and Richadson	20.57	21.95	0.02
	Qu	15.66	15.93	1.33

The experimental outcomes of the settlement drag coefficient of Newtonian fluid perfectly align with the predicted outcomes of various models, and the average error is within 5% (Table 4). However, the error between the experimental value and the anticipated one of spherical particles in NNF is relatively large. In power-law fluid (PLF), the MRE between the experimental result and the predicted value of each model is 9.62%, 10.61%, 10.78% and 12.57% respectively, while in HBF, the MRE is 20.57% and 15.66% respectively. Due to the large error, the existing C_D-Re_N relation expression for the SDCSPs cannot be directly used for NNFs. Therefore, it's necessary to establish a new mode for accurately anticipating the SDCSPs in NNFs.

Cheng (2009) [20] proposed a widely used relation expression of settlement drag coefficient, which is an empirical function of Reynolds number (Re_N):

$$C_{D,sph} = \frac{24}{Re_N}(1 + A Re_N)^B + C\left[1 - \exp(-D Re_N^E)\right] \tag{9}$$

in which E, D, C, B and A are all correlation coefficients, dimensionless, and $C_{D,sph}$ are settlement drag coefficients of spherical particles.

By fitting the experimental data, the anticipation mode of SDC C_D-Re_N of SPs in NF, PLF and HBF is finally regressed, as shown in formula (10). The comparison between the predicted value of spherical particle C_D and the experimental data is shown in Figure 8.

Figure 8 uses a log coordinate axis, where the abscissa is the experimental measured value of the spherical particles in the fluid, and the ordinate is the predicted value of the model. The calculated results of formula (10) perfectly align with the experimental data. By comparing the predicted values and experimental values of Newtonian fluid (Figure 8a), PLF (Figure 8b) and HBF (Figure 8c), the MREs between the predicted values and experimental ones of the mode proposed in the study are 3.10%, 5.39% and 3.73%, which are lower than the predicted values of previous models in Table 4; it means that the proposed model can well predict the settlement drag coefficient of spherical particles (SDCSPs) in fluids with different rheological models.

$$\begin{cases} C_{D,sph} = \frac{24}{\mathrm{Re}_N}(1+1.197\mathrm{Re}_N)^{0.161} + 0.663\left[1-\exp(-0.229\mathrm{Re}_N^{1.032})\right] (a) \\ C_{D,sph} = \frac{24}{\mathrm{Re}_N}(1+0.987\mathrm{Re}_N)^{0.228} + 0.217\left[1-\exp(-0.983\mathrm{Re}_N^{0.263})\right] (b) \\ C_{D,sph} = \frac{24}{\mathrm{Re}_N}(1+0.200\mathrm{Re}_N)^{0.215} + 0.168\left[1-\exp(-0.529\mathrm{Re}_N^{0.991})\right] (c) \end{cases} \quad (10)$$

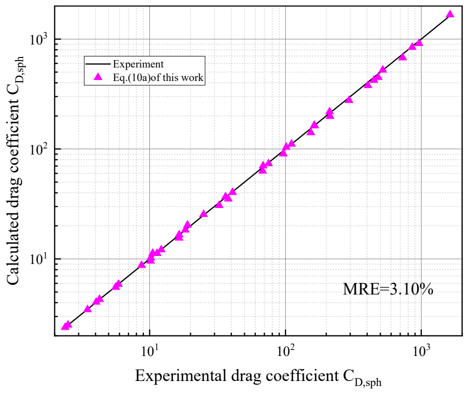

(**a**)

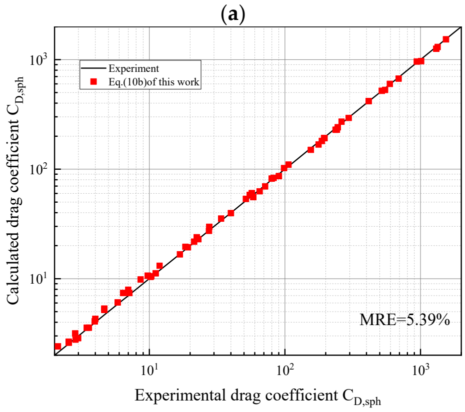

(**b**)

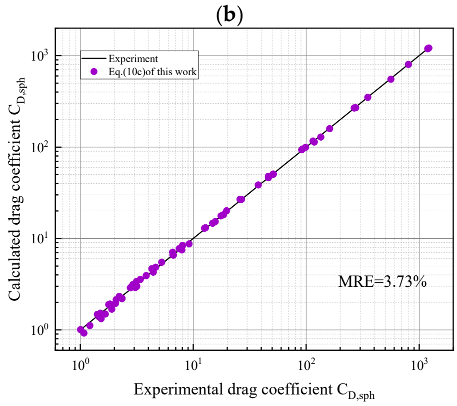

(**c**)

Figure 8. Comparison between predicted value and experimental data of CD of spherical particles: (**a**) NF; (**b**) PLF; (**c**) HBF.

3.2. Drag Coefficient of NSPs

The irregular NSPs shape will greatly affect the exerted drag force by the fluid, like rock debris and proppant, thus changing their final settlement speed. Therefore, considering the particle shape impact, the circularity C is introduced, and the correlation formula of the settlement coefficient of NSPs, $C_{D,irregular}$, is proposed:

$$C_{D,irregular} = C_{D,sph} \exp[\alpha \mathrm{Re}_N^{\beta}(1-c)^{\lambda}] \tag{11}$$

where $C_{D,\ irregular}$ is the SDCNPs; α, β and λ represents the correlation coefficient, dimensionless.

Similarly, though fitting the experimental data of non-spherical sand settlement, the parameters in formula (11) can be obtained, substitute them into formula (10), then the expression of sand settlement drag coefficient $C_{D,irregular}$ is as follows:

$$\begin{cases} C_{D,irregular} = \left(\frac{24}{\mathrm{Re}_N}(1+1.197\mathrm{Re}_N)^{0.161} + 0.663\left[1-\exp(-0.229\mathrm{Re}_N^{1.032})\right]\right)\exp[1.230\mathrm{Re}_N^{0.038}(1-c)^{0.040}](a) \\ C_{D,irregular} = \left(\frac{24}{\mathrm{Re}_N}(1+0.987\mathrm{Re}_N)^{0.228} + 0.217\left[1-\exp(-0.983\mathrm{Re}_N^{0.263})\right]\right)\exp[1.382\mathrm{Re}_N^{0.004}(1-c)^{0.063}](b) \\ C_{D,irregular} = \left(\frac{24}{\mathrm{Re}_N}(1+0.200\mathrm{Re}_N)^{0.215} + 0.168\left[1-\exp(-0.529\mathrm{Re}_N^{0.991})\right]\right)\exp[1.319\mathrm{Re}_N^{0.046}(1-c)^{0.012}](c) \end{cases} \tag{12}$$

By comparing the predicted and experimental values of Newtonian fluid (Figure 9)), PLF (Figure 9b) and HBF (Figure 9c), the calculated results of formula (12) perfectly align with the experimental data. The errors between the anticipated and experimental values of the mode presented in the investigation are 5.70%, 6.24% and 6.72%, respectively.

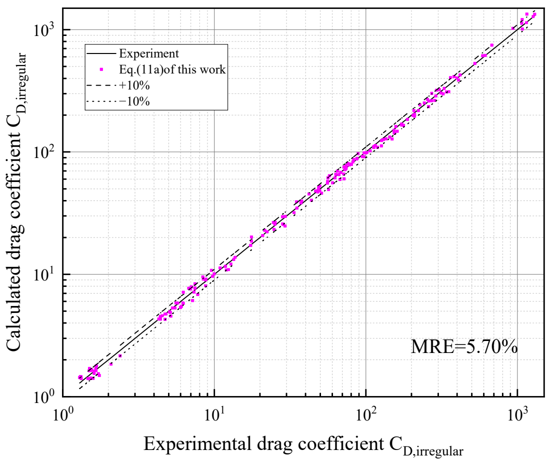

(**a**)

Figure 9. *Cont.*

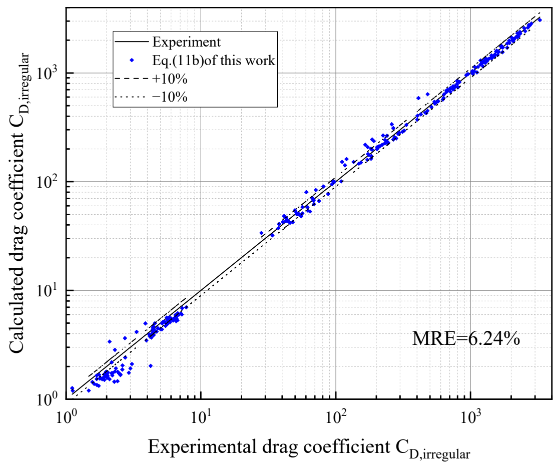

(**b**)

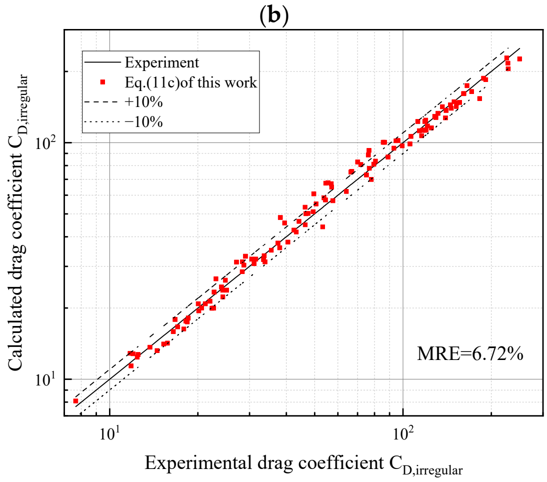

(**c**)

Figure 9. Comparison between anticipated C_D value of NSPs and experimental data: (**a**) NF; (**b**) PLF; (**c**) HBF.

4. Conclusions

The settling features of NSPs and SPs in different fluids are studied experimentally. In order to expand the experimental data and scope of application, the Newton, Herschel-Bulkley and Power-law fluids (PLFs) were selected in experimental fluids. A new formula for computing the SDCSPs in NF and NNF is proposed by modifying the correlations proposed by Cheng (2009). According to the anticipation mode of the drag coefficient of SPs, and introducing the shape factor circularity c, which is easier to determine, the settlement drag coefficient model of NSPs in NF and NNF is proposed. The Reynolds number of the proposed model is 0.01–158 and the circularity is 0.348–1. The predicted values perfectly align with experimental values, and the average relative errors are 5.70%, 6.24% and 6.72%, respectively. This work can provide a valuable reference for proppant migration cuttings settlement researchers; it should be noted that this study has certain limitations because only Newton, Herschel-Bulkley and Power-law fluids are considered. Therefore, in future research, other types of fluids will be combined and modified with this model, and there will be a more accurate understanding of the settlement characteristics of irregular particles in non-Newtonian fluids.

Author Contributions: Writing—review and editing, J.L.; writing—original draft preparation, Z.H.; conceptualization, G.X.; investigation, L.Y. All authors have read and agreed to the published version of the manuscript.

Funding: The authors express their appreciation to the Fund Project: basic research program on deep petroleum resource accumulation and key engineering technologies (No: U19B6003) of Sinopec Research Institute of Petroleum Engineering Co., Ltd.

Conflicts of Interest: On behalf of all the co-authors, the corresponding author declares no conflict of interest.

References

1. Awad, A.M.; Hussein, I.A.; Nasser, M.S.; Karami, H.; Ahmed, R. CFD modeling of particle settling in drilling fluids: Impact of fluid rheology and particle characteristics. *J. Pet. Sci. Eng.* **2021**, *199*, 108326. [CrossRef]
2. Qu, J.; Yan, T.; Sun, X.; Li, Z.; Li, W. Decaying swirl flow and particle behavior through the hole cleaning device for horizontal drilling of fossil fuel. *Energies* **2019**, *12*, 336. [CrossRef]
3. Zhang, G.; Gutierrez, M.; Chao, K. Hydrodynamic and mechanical behavior of multi-particle confined between two parallel plates. *Adv. Powder Technol.* **2019**, *30*, 439–450. [CrossRef]
4. Stokes, G.G. On the effect of the internal friction of fluids in the motion of pendulums. *Trans. Cambridge Philos. Soc.* **1851**, *9*, 8–106.
5. Abraham, F.F. Functional dependence of drag coefficient of a sphere on Reynolds number. *Phys. Fluids* **1970**, *13*, 2194–2195. [CrossRef]
6. Clift, R.; Gauvin, W.H. Motion of entrained particles in gas streams. *Can. J. Chem. Eng.* **1971**, *49*, 439–448. [CrossRef]
7. Brown, P.P.; Lawler, D.F. Sphere drag and settling velocity revisited. *J. Environ. Eng.* **2003**, *129*, 222–231. [CrossRef]
8. Terfous, A.; Hazzab, A.; Ghenaim, A. Predicting the drag coefficient and settling velocity of spherical particles. *Powder Technol.* **2013**, *239*, 12–20. [CrossRef]
9. Agwu, O.E.; Akpabio, J.U.; Alabi, S.B.; Dosunmu, A. Settling velocity of drill cuttings in drilling fluids: A review of experimental, numerical simulations and artificial intelligence studies. *Powder Technol.* **2018**, *339*, 728–746. [CrossRef]
10. Goossens, W.R.A. Review of the empirical correlations for the drag coefficient of rigid spheres. *Powder Technol.* **2019**, *352*, 350–359. [CrossRef]
11. Yao, S.; Chang, C.; Hai, K.; Huang, H.; Li, H. A review of experimental studies on the proppant settling in hydraulic fractures. *J. Pet. Sci. Eng.* **2022**, *208*, 109211. [CrossRef]
12. Chhabra, R.P. Motion of spheres in power law (viscoinelastic) fluids at intermediate Reynolds numbers: A unified approach. *Chem. Eng. Process. Process Intensif.* **1990**, *28*, 89–94. [CrossRef]
13. Lali, A.M.; Khare, A.S.; Joshi, J.B.; Nigam, K.D.P. Behaviour of solid particles in viscous non-Newtonian solutions: Settling velocity, wall effects and bed expansion in solid-liquid fluidized beds. *Powder Technol.* **1989**, *57*, 39–50. [CrossRef]
14. Kelessidis, V.C. Terminal velocity of solid spheres falling in Newtonian and non-Newtonian liquids. *Tech. Chron. Sci. J. TCG* **2003**, *5*, 43–54.
15. Shah, S.N.; El Fadili, Y.; Chhabra, R.P. New model for single spherical particle settling velocity in power law (visco-inelastic) fluids. *Int. J. Multiph. Flow* **2007**, *33*, 51–66. [CrossRef]
16. Peden, J.M.; Luo, Y. Settling velocity of variously shaped particles in drilling and fracturing fluids. *SPE Drill. Eng.* **1987**, *2*, 337–343. [CrossRef]
17. Kelessidis, V.C.; Mpandelis, G. Measurements and prediction of terminal velocity of solid spheres falling through stagnant pseudoplastic liquids. *Powder Technol.* **2004**, *147*, 117–125. [CrossRef]
18. Turton, R.; Levenspiel, O. A short note on the drag correlation for spheres. *Powder Technol.* **1986**, *47*, 83–86. [CrossRef]
19. Haider, A.; Levenspiel, O. Drag coefficient and terminal velocity of spherical and nonspherical particles. *Powder Technol.* **1989**, *58*, 63–70. [CrossRef]
20. Cheng, N.S. Comparison of formulas for drag coefficient and settling velocity of spherical particles. *Powder Technol.* **2009**, *189*, 395–398. [CrossRef]
21. Song, X.; Xu, Z.; Li, G.; Pang, Z.; Zhu, Z. A new model for predicting drag coefficient and settling velocity of spherical and non-spherical particle in Newtonian fluid. *Powder Technol.* **2017**, *321*, 242–250. [CrossRef]
22. Okesanya, T.; Abdukarimov, A.; Kuru, E. Generalized models for predicting the drag coefficient and settling velocity of rigid spheres in viscoelastic and viscoinelastic power-law fluids. *J. Pet. Sci. Eng.* **2020**, *191*, 107077. [CrossRef]
23. Khan, A.R.; Richardson, J.F. The resistance to motion of a solid sphere in a fluid. *Chem. Eng. Commun.* **1987**, *62*, 135–150. [CrossRef]
24. Zhang, G.; Li, M.; Geng, K.; Han, R.; Xie, M.; Liao, K. New integrated model of the settling velocity of proppants falling in viscoelastic slick-water fracturing fluids. *J. Nat. Gas Sci. Eng.* **2016**, *33*, 518–526. [CrossRef]
25. Padhy, S.; Rodriguez, M.; Shaqfeh, E.; Iaccarino, G.; Morris, J.; Tonmukayakul, N. The effect of shear thinning and walls on the sedimentation of a sphere in an elastic fluid under orthogonal shear. *J. Non-Newton. Fluid Mech.* **2013**, *201*, 120–129. [CrossRef]
26. Williams, G.P. Particle roundness and surface texture effects on fall velocity. *J. Sediment. Petrol.* **1997**, *36*, 255–259. [CrossRef]
27. Wadell, H. The coefficient of resistance as a function of Reynolds number for solids of various shapes. *J. Frankl. Inst.* **1934**, *217*, 459–490. [CrossRef]
28. Tran-Cong, S.; Gay, M.; Michaelides, E.E. Drag coefficients of irregularly shaped particles. *Powder Technol.* **2004**, *139*, 21–32. [CrossRef]

29. Corey, A.T. Influence of the Shape on the Fall Velocity of Sand Grains. Ph.D. Thesis, Colorado State University, Fort Collins, CO, USA, 1949.
30. Bouwman, A.M.; Bosma, J.C.; Vonk, P.; Wesselingh, J.H.A.; Frijlink, H.W. Which shape factor (s) best describe granules? *Powder Technol.* **2004**, *146*, 66–72. [CrossRef]
31. Hölzer, A.; Sommerfeld, M. New simple correlation formula for the drag coefficient of non-spherical particles. *Powder Technol.* **2008**, *184*, 361–365. [CrossRef]
32. Wang, Y.; Zhou, L.; Wu, Y.; Yang, Q. New simple correlation formula for the drag coefficient of calcareous sand particles of highly irregular shape. *Powder Technol.* **2018**, *326*, 379–392. [CrossRef]
33. Chien, S.F. Settling velocity of irregularly shaped particles. *SPE Drill. Complet.* **1994**, *9*, 281–289. [CrossRef]
34. Dioguardi, F.; Mele, D. A new shape dependent drag correlation formula for non-spherical rough particles. *Exp. Results. Powder Technol.* **2015**, *277*, 222–230. [CrossRef]
35. Xu, Z.; Song, X.; Li, G.; Pang, Z.; Zhu, Z. Settling behavior of non-spherical particles in power-law fluids: Experimental study and model development. *Particuology* **2019**, *46*, 30–39. [CrossRef]
36. Rushd, S.; Hafsa, N.; Al-Faiad, M.; Arifuzzaman, M. Modeling the settling velocity of a sphere in Newtonian and non-Newtonian fluids with machine-learning algorithms. *Symmetry* **2021**, *13*, 71. [CrossRef]
37. Barati, R.; Neyshabouri, S.A.A.S.; Ahmadi, G. Development of empirical models with high accuracy for estimation of drag coefficient of flow around a smooth sphere: An evolutionary approach. *Powder Technol.* **2014**, *257*, 11–19.
38. Akanni, O.; Fu, C.; Guo, B. Drag Coefficients of Irregularly Shaped Particles in Newtonian Fluids. *Sustainability* **2021**, *13*, 7517. [CrossRef]
39. Gavrilov, A.A.; Finnikov, K.A.; Podryabinkin, E.V. Modeling of steady Herschel–Bulkley fluid flow over a sphere. *J. Eng. Thermophys.* **2017**, *26*, 197–215. [CrossRef]
40. Zhou, C.; Su, J.; Chen, H.; Shi, Z. Terminal velocity and drag coefficient models for disc-shaped particles based on the imaging experiment. *Powder Technol.* **2022**, *398*, 117062. [CrossRef]
41. Okesanya, T.; Kuru, E.; Sun, Y. A New Generalized Model for Predicting the Drag Coefficient and the Settling Velocity of Rigid Spheres in Viscoplastic Fluids. *SPE J.* **2020**, *25*, 3217–3235. [CrossRef]
42. Yan, T.; Qu, J.Y.; Sun, X.F.; Li, W.; Chen, Y.; Hu, Q.B. A novel predictive model of drag coefficient and settling velocity of drill cuttings in non-Newtonian drilling fluids. *Pet. Sci.* **2021**, *18*, 1729–1738. [CrossRef]